

# A parameterization of ion-induced nucleation of sulphuric acid and water for atmospheric conditions

M. S. Modgil

Department of Physics, Indian Institute of Technology, Kanpur, India

Sanjeev Kumar and S. N. Tripathi

Department of Civil Engineering, Indian Institute of Technology, Kanpur, India

E. R. Lovejoy

NOAA Aeronomy Laboratory, Boulder, Colorado, USA

Received 29 September 2004; revised 19 January 2005; accepted 2 May 2005; published 12 October 2005.

[1] This paper describes a five-dimensional parameterization of ion-induced nucleation (IIN) that covers the complete range of conditions relevant to the lower atmosphere. The parameters are (1) temperature  $T$  (190–300 K), (2) relative humidity RH (0.05–0.95), (3) number concentration of  $\text{H}_2\text{SO}_4$  ( $10^5$ – $10^8$   $\text{cm}^{-3}$ ), (4) first-order loss of  $\text{H}_2\text{SO}_4$  to particles ( $0.00009$ – $0.0245$   $\text{s}^{-1}$ ), and (5) ion source rate ( $2$ – $50$  ion pairs  $\text{cm}^{-3}$   $\text{s}^{-1}$ ). The parameterization is based on a steady state version of the kinetic aerosol model Sulphuric Acid and Water Nucleation (SAWNUC) that uses experimentally measured thermodynamics for the ion clusters. Parameterized formulas are obtained for the following variables: (1) particle nucleation rate ( $\text{cm}^{-3}$   $\text{s}^{-1}$ ), (2)  $\text{H}_2\text{SO}_4$  nucleation rate ( $\text{cm}^{-3}$   $\text{s}^{-1}$ ), (3) number of  $\text{H}_2\text{SO}_4$  molecules in average nucleating cluster, (4) number of  $\text{H}_2\text{O}$  molecules in average nucleating cluster, and (5) radius (nanometers) of average nucleating cluster. The parameterization generally reproduces the modeled nucleation rate to within an order of magnitude over the whole range of conditions, except when the nucleation rate is very low ( $<10^{-6}$   $\text{cm}^{-3}$   $\text{s}^{-1}$ ), which corresponds to a rate of less than  $0.1$  particle  $\text{d}^{-1}$   $\text{cm}^{-3}$ . This parameterization speeds up IIN calculations by a factor of  $\sim 10^6$ , as compared to the original SAWNUC model.

**Citation:** Modgil, M. S., S. Kumar, S. N. Tripathi, and E. R. Lovejoy (2005), A parameterization of ion-induced nucleation of sulphuric acid and water for atmospheric conditions, *J. Geophys. Res.*, *110*, D19205, doi:10.1029/2004JD005475.

## 1. Introduction

[2] Aerosol is ubiquitous in Earth's atmosphere, and affects health, visibility, atmospheric chemistry, and climate [Kulmala, 2003]. Gas phase nucleation is an important source of aerosol in Earth's atmosphere [Kulmala, 2003]. However, the specific mechanisms of atmospheric nucleation are uncertain. Ions are likely aerosol precursors because the charge greatly stabilizes the small clusters with respect to evaporation. A number of modeling studies [Raes and Janssens, 1986; Kim *et al.*, 1997; Yu and Turco, 2000, 2001; Kulmala *et al.*, 2000; Laakso *et al.*, 2002] have shown that ion-induced nucleation is potentially important in the atmosphere. However, the predictions of these studies have considerable uncertainty because they are based either on the liquid drop model thermodynamics or estimates of cluster kinetics. Lovejoy *et al.* [2004] have recently developed a model (SAWNUC) of ion-induced nucleation of  $\text{H}_2\text{SO}_4$  and  $\text{H}_2\text{O}$  that is based on measured thermodynamics of small ion clusters. This model appears to reproduce

observations of ultra fine particle formation in the middle and upper troposphere [Lovejoy *et al.*, 2004], as well as the lower stratosphere [Lee *et al.*, 2003]. However, the model could not explain the observed particle nucleation in the lower troposphere.

[3] Here we present a parameterization of the output of SAWNUC [Lovejoy *et al.*, 2004]. A relationship is given relating the ion-induced nucleation rate (formation of new neutral particles larger than the critical cluster by way of ion-induced nucleation) as a function of temperature, RH,  $\text{H}_2\text{SO}_4$  concentration, ion source rate and first-order loss of  $\text{H}_2\text{SO}_4$  to preexisting aerosol.

[4] Similar parameterizations of neutral nucleation rates have been published. Vehkamäki *et al.* [2002] parameterized the critical nucleus composition, critical cluster radii and homogenous nucleation rates for the neutral sulphuric acid/water system on the basis of classical nucleation theory. The Vehkamäki *et al.* [2002] parameterized values compare well with theory, for  $\text{RH} > 0.3$ ,  $230 < T < 305$  K,  $10^4 < \text{H}_2\text{SO}_4 < 10^{11}$   $\text{cm}^{-3}$ , nucleation rates between  $10^{-7}$  and  $10^{10}$   $\text{cm}^{-3}$   $\text{s}^{-1}$ , and critical cluster containing at least four molecules. Napari *et al.* [2002] published a parameterization of the neutral

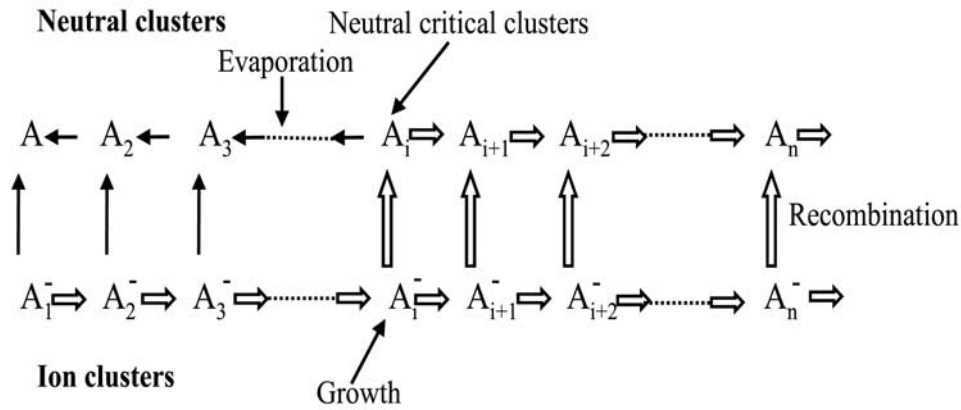


**Figure 1.** Ion-induced nucleation mechanism. In this example, the neutral nucleation pathway is inhibited because of a barrier on the Gibbs free energy surface. Clusters smaller than the critical cluster preferentially evaporate whereas clusters larger than the critical cluster grow. The ion cluster growth is spontaneous and competes with recombination (vertical arrows). Recombination that produces a neutral particle larger than the critical cluster leads to nucleation. This process is indicated by the large arrows.

ternary  $\text{H}_2\text{O}/\text{H}_2\text{SO}_4/\text{NH}_3$  nucleation rates based on classical nucleation theory for atmospheric conditions.

## 2. Model

[5] SAWNUC [Lovejoy *et al.*, 2004] is a kinetic model of ion-induced nucleation (IIN) that is based on experimental thermodynamics of small ion clusters of  $\text{H}_2\text{SO}_4$  and  $\text{H}_2\text{O}$ . The pathway for IIN involves ion cluster growth followed by recombination that produces a stable neutral cluster, larger than the critical cluster. This is an effective mechanism to bypass a neutral nucleation barrier (Figure 1). In classical nucleation theory, the thermodynamics of clusters are approximated with the liquid drop model [Seinfeld and Pandis, 1998], which is inappropriate for small molecular clusters, and leads to large uncertainties in nucleation rates. Lovejoy *et al.* [2004] measured the thermodynamics for the growth and evaporation of small cluster ions containing  $\text{H}_2\text{SO}_4$  and  $\text{H}_2\text{O}$ , and incorporated these data into a kinetic aerosol model to yield predictions of the rate of ion-induced nucleation for atmospheric conditions. Large cluster thermodynamics are treated with the Thomson equation and the intermediate cluster thermodynamics are interpolated. Experimental studies indicate that the positive ions are less likely to nucleate than the negative ions [Froyd and Lovejoy, 2003a, 2003b; Wilhelm *et al.*, 2004]. Accordingly, the positive ions are treated as a single species, and the neutral and negative ions are treated explicitly. For the neutral and negative clusters, the model uses 20–40 bins that increment by one sulphuric acid molecule, representing hydrated  $(\text{H}_2\text{SO}_4)_n$  and  $\text{HSO}_4^-(\text{H}_2\text{SO}_4)_{n-1}$ , respectively. In the next 40–60 bins the number of sulphuric molecules increases geometrically, typically by a factor of 1.5 in order to account for particles up to about  $1 \mu\text{m}$  diameter. All clusters equilibrate with water and grow and evaporate by addition and loss of  $\text{H}_2\text{SO}_4$ . Negative clusters coagulate with neutral clusters, recombine with positive ions, and are formed by the coagulation of smaller neutral and negative clusters. Neutral clusters coagulate with neutral and negative clusters, and are formed by recombination of ion clusters as well as by coagulation of neutrals clusters.

[6] The ion-induced nucleation rate (new particles per volume per time) is defined as the rate of formation of stable (i.e., larger than the critical cluster) neutral clusters by recombination of ionic clusters. In SAWNUC this was implemented as the rate of recombination of ion clusters larger than the neutral critical cluster minus a small loss of the neutral clusters due to reaction with ion clusters.

$$J_{\text{IIN}} = \sum_{I > \text{c.c.}} k_r [I] [\text{pos}] - \sum_{I > \text{c.c.}} \sum_J k_{i,j}^c [i] [J] \quad (1)$$

where  $k_r$  is the recombination rate coefficient,  $[I]$  is the concentration of ion clusters in bin  $I$ ,  $[\text{pos}]$  is the concentration of positive ions, and  $k_{i,j}^c$  is the coagulation rate coefficient for reaction between neutral cluster  $i$  and ion cluster  $J$ . It is assumed that the positive ions do not contain  $\text{H}_2\text{SO}_4$ . It is clear that the conventional definition of the nucleation rate does not apply to IIN because the IIN mechanism is significantly different from the standard neutral scheme. We defined the production rate of new neutral particles of a specified average size so that the parameterization could be easily coupled to a standard aerosol microphysical model. The larger charged clusters are in steady state with the corresponding neutrals. The ions recombine to produce the neutrals and the neutrals are charged to remake the ions. At steady state, these rates are the same. Equation (1) includes both the recombination and the charging rates, and hence, for the larger charged particles/clusters, their neutralization is not counted as nucleation. The  $\text{H}_2\text{SO}_4$  nucleation rate ( $\text{H}_2\text{SO}_4$  molecules per volume per time) is defined as the net rate of consumption of  $\text{H}_2\text{SO}_4$  due to the formation of new particles

$$R_{\text{H}_2\text{SO}_4} = \sum_{I > \text{c.c.}} n_I k_r [I] [\text{pos}] - \sum_{I > \text{c.c.}} \sum_J n_i k_{i,j}^c [i] [J] \quad (2)$$

where  $n_I$  is the number of  $\text{H}_2\text{SO}_4$  molecules in ion cluster  $I$  and  $n_i$  is the number of  $\text{H}_2\text{SO}_4$  molecules in neutral cluster  $i$ . The average number of  $\text{H}_2\text{SO}_4$  molecules in the nucleating

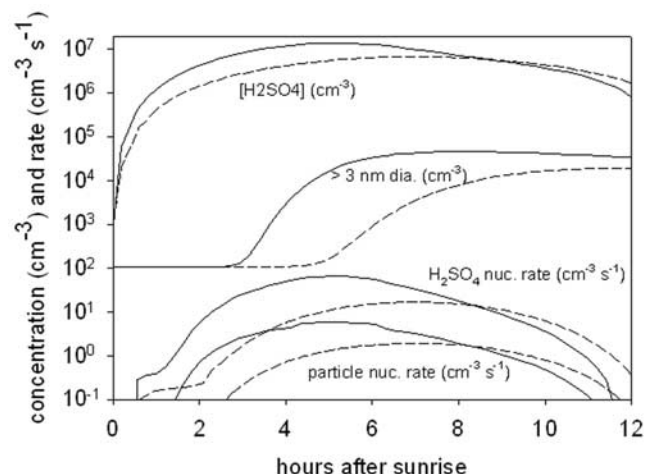


**Figure 2.** SAWNUC output for 240 K, 307 mbar, RH = 0.5, 15 ion pairs  $\text{cm}^{-3} \text{s}^{-1}$ ,  $2 \mu\text{m}^2 \text{cm}^{-3}$ , 12 hours of daylight, and  $\text{H}_2\text{SO}_4$  peak noontime source rates of 1000 (dashed lines) and  $3000 \text{cm}^{-3} \text{s}^{-1}$  (solid lines). The instantaneous nucleation rates are calculated with equations (1) and (2).

clusters is given by the ratio of the  $\text{H}_2\text{SO}_4$  nucleation rate to the particle nucleation rate

$$\bar{N}_{\text{H}_2\text{SO}_4} = \frac{R_{\text{H}_2\text{SO}_4}}{J_{\text{IIN}}} \quad (3)$$

The average size of the nucleating particles is determined by equilibrating water with a cluster containing the average number of  $\text{H}_2\text{SO}_4$  molecules.

[7] SAWNUC calculates the temporal evolution of ion and neutral clusters for a given a set of conditions ( $T$ , RH,  $\text{H}_2\text{SO}_4$  production rate, ion production rate, etc.). The  $\text{H}_2\text{SO}_4$  production is modeled as a half sine wave during daylight hours and zero at night. Figure 2 shows the calculated profiles of  $[\text{H}_2\text{SO}_4]$  and ultrafine particles versus time for a given set of conditions ( $T = 240 \text{ K}$ , RH = 0.5, 15 ion pairs  $\text{cm}^{-3} \text{s}^{-1}$ ,  $2 \mu\text{m}^2 \text{cm}^{-3}$  of 30 nm radius particles at  $t = 0$ , peak noontime  $\text{H}_2\text{SO}_4$  production rates equal to 1000 and  $3000 \text{cm}^{-3} \text{s}^{-1}$ , 12 hours of daylight). Also shown are the instantaneous particle and  $\text{H}_2\text{SO}_4$  nucleation rates throughout the day (equations (1) and (2)). Ideally, a parameterization should give the instantaneous nucleation rate as a function of the ambient conditions. Here we show that the instantaneous nucleation rates are given to a good approximation by the steady state values. SAWNUC was modified to run until steady state with a constant  $[\text{H}_2\text{SO}_4]$ . The integration time was chosen as  $t(\text{s}) = 1.0 \times 10 / [\text{H}_2\text{SO}_4](\text{molec. cm}^{-3}) + 3/(qk_r)^{1/2}$  which assured that the nucleation kinetics were in steady state. A plot of the calculated steady state and instantaneous particle nucleation rate versus  $[\text{H}_2\text{SO}_4]$  for the conditions of Figure 2 are shown in Figure 3. There is excellent agreement over many orders of magnitude of nucleation rate.

[8] A steady state, nested do loop version, of SAWNUC was created, in which the five input variables were (1) temperature  $T$  (190–300 K), (2) relative humidity RH (0.05–0.95), (3) number concentration of  $\text{H}_2\text{SO}_4$

( $10^5$ – $10^8 \text{cm}^{-3}$ ), (4) preexisting aerosol surface area SA ( $2$ – $100 \mu\text{m}^2 \text{cm}^{-3}$ ), and (5) ion source  $q$  ( $1$ – $50 \text{cm}^{-3} \text{s}^{-1}$ ). Six output variables generated from SAWNUC were (1) particle nucleation rate ( $h_1, \text{cm}^{-3} \text{s}^{-1}$ ), (2) nucleating  $\text{H}_2\text{SO}_4$  rate ( $h_2, \text{cm}^{-3} \text{s}^{-1}$ ), (3) number of  $\text{H}_2\text{SO}_4$  molecules in average nucleating cluster ( $h_3$ ), (4) number of  $\text{H}_2\text{O}$  molecules in average nucleating cluster ( $h_4$ ), (5) radius of average nucleating cluster ( $h_5, \text{nm}$ ), and (6) first-order loss of  $\text{H}_2\text{SO}_4$  to particles ( $h_6$ ). This steady state, nested loop version of SAWNUC, was used to generate the data required in the parameterization of IIN. The first-order loss of  $\text{H}_2\text{SO}_4$  to particles is defined as

$$h_6 = \sum_i k_{i,\text{H}_2\text{SO}_4}^c [i] + \sum_I k_{I,\text{H}_2\text{SO}_4}^c [I] \quad (4)$$

where  $k_{i,\text{H}_2\text{SO}_4}^c$  is the second-order rate coefficient for uptake of  $\text{H}_2\text{SO}_4$  by cluster  $i$ .

### 3. Parameterization

[9] In this section we describe the parameterization process, used to parameterize the output data set from SAWNUC.

#### 3.1. Grid Effect

[10] Discretization of the complete range of atmospheric conditions, as input to SAWNUC, was required. Because of the comparatively large number of variables in the input data set, namely five, the size of input data set becomes large very quickly, as the number of grid points is increased. Parameterization of output data set from SAWNUC, for large grids, was thus constrained by computational resources. This implied memory related problems, e.g., the size of RAM, or RAM addressable by the operating system. The parameterization had to be achieved within the

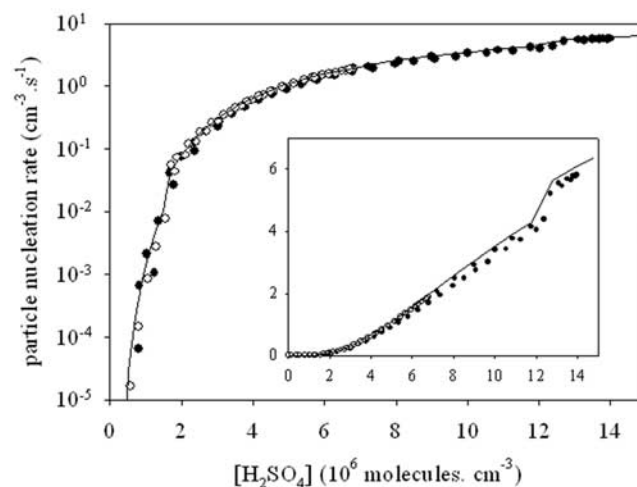


**Figure 3.** Particle nucleation rate as a function of  $[\text{H}_2\text{SO}_4]$  for the conditions of Figure 2. The points are the instantaneous rates, where open circles are for 1000 and solid circles are for  $3000 \text{H}_2\text{SO}_4 \text{cm}^{-3} \text{s}^{-1}$  at noon. The solid lines are calculated with the steady state version of SAWNUC as described in the text. Inset is the same data on a linear scale.

constraint of available computational resources, which in this case were, a Pentium 4 processor with a clock speed of 2.6 GHz, and 1 GB RAM.

[11] One of the primary steps in the study was optimization of the input nested do loop grid to SAWNUC, so that resulting efficiency of parameterization was high. We define efficiency of parameterization, as the percentage of points where the ratio of the “model value” to the “parameterized value” falls between 0.5 and 2. This required determining, which variables required a relatively fine grid and for which ones a coarse grid would suffice. After a large number of iterations of this process, it turned out that a finer discretization was required for temperature and relative humidity. Higher resolution was required because the IIN rate is most sensitive to temperature and relative humidity. Concentration of sulphuric acid, surface area, and ion source could be modeled, with a relatively coarse grid. Within the limitation of our computational resource, the final grid that has been used for parameterization had  $20 \times 15 \times 8 \times 4 \times 8 = 76,800$  points, where there were 20 points for temperature, 15 for relative humidity, 8 for concentration of sulphuric acid, 4 for preexisting surface area, and 8 for ion source.

[12] The output data set from SAWNUC was filtered to remove data points with very low values of particle nucleation rate ( $h_1 < 10^{-6} \text{ cm}^{-3} \text{ s}^{-1}$ ). This reduced the number of data points for the parameterization to 40,728. The parameterized functions presented here are strictly valid for those atmospheric conditions giving a particle nucleation rate of  $h_1 > 10^{-6} \text{ cm}^{-3} \text{ s}^{-1}$ . The relevant ranges

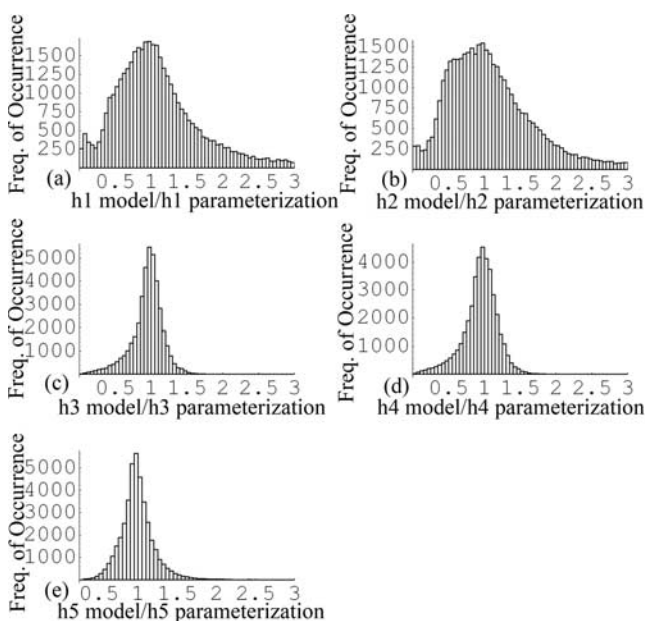


**Figure 4.** Efficiency plots for (a) particle nucleation rate ( $h_1$ ), (b) nucleating sulphuric acid rate ( $h_2$ ), (c) number of sulphuric acid molecules in the average nucleating cluster ( $h_3$ ), (d) number of water molecules in the average nucleating cluster ( $h_4$ ), and (e) radius of average nucleating cluster ( $h_5$ ), showing ratio of model value to parameterized value on the  $x$  axis and corresponding frequency of occurrence on the  $y$  axis.

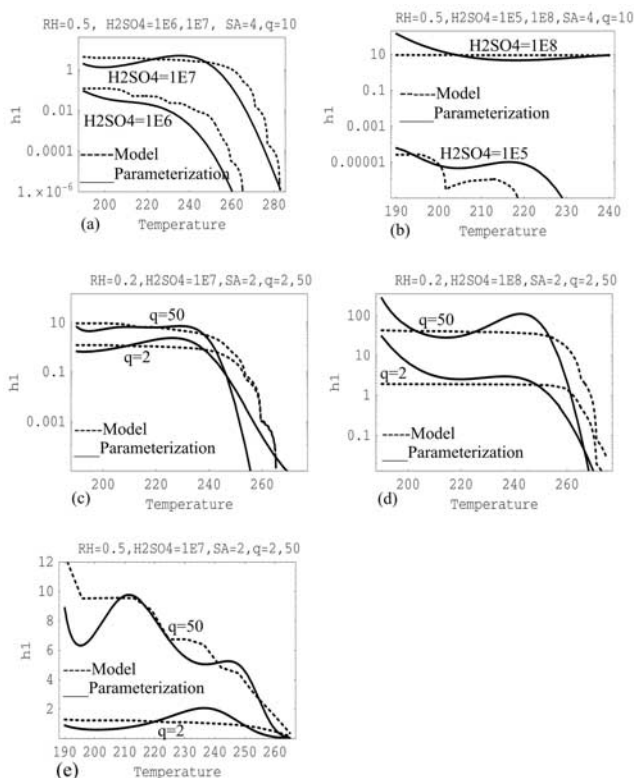


**Figure 5.** (a) Comparison of modeled and parameterized particle nucleation rate ( $h_1$ ) for  $\text{RH} = 0.5$ ,  $\text{H}_2\text{SO}_4 = 10^6$  and  $10^7 \text{ cm}^{-3}$ ,  $\text{SA} = 4 \mu\text{m}^2 \text{ cm}^{-3}$ , and ion source equal to  $10 \text{ cm}^{-3} \text{ s}^{-1}$ . (b) Same as Figure 5a except for  $\text{H}_2\text{SO}_4 = 10^5$  and  $10^8 \text{ cm}^{-3}$ . (c) Comparison of modeled and parameterized particle nucleation rate for  $\text{RH} = 0.2$ ,  $\text{H}_2\text{SO}_4 = 10^7 \text{ cm}^{-3}$ ,  $\text{SA} = 2 \mu\text{m}^2 \text{ cm}^{-3}$ , and ion source equal to 2.0 and  $50.0 \text{ cm}^{-3} \text{ s}^{-1}$ . (d) Same as Figure 5c except for  $\text{H}_2\text{SO}_4 = 10^8 \text{ cm}^{-3}$ . (e) Same as Figure 5c except for  $\text{RH} = 0.5$ .

of atmospheric conditions ( $T$ ,  $\text{RH}$ ,  $\text{H}_2\text{SO}_4$ ,  $h_6$ ,  $q$ ) can be visualized with three-dimensional (3-D) plots<sup>1</sup> of the model output.<sup>1</sup>

### 3.2. Basis Functions

[13] A smooth differentiable function  $f = f(x, y, z, \dots)$  of independent variables ( $x, y, z, \dots$ ) can be approximated as a truncated Taylor series. This truncated Taylor series is a multidimensional polynomial of variables ( $x, y, z, \dots$ ), with partial derivatives  $f_x = \partial f / \partial x$ , etc. appearing as coefficients. One approach to parameterization would be to use a multivariable polynomial, consisting of powers of independent variables ( $x, y, z, \dots$ ), as basis functions, and determine the coefficients (partial derivatives,  $f_x, f_y, f_z, \dots$ , etc., in this case), in the truncated Taylor series expansion. Mathematica, a numerical and symbolic computational language, is used for the parameterization.

[14] A least squares fit, to a data set, as a linear combination of functions, of independent variables was used to arrive at an initial parameterization of IIN, in which polynomials consisting of powers of the five input variables ( $T$ ,  $\text{RH}$ ,  $\text{H}_2\text{SO}_4$ ,  $h_6$ ,  $q$ ) were used as basis functions and

<sup>1</sup>Auxiliary material is available at <ftp://ftp.agu.org/apend/jd/2004JD005475>.

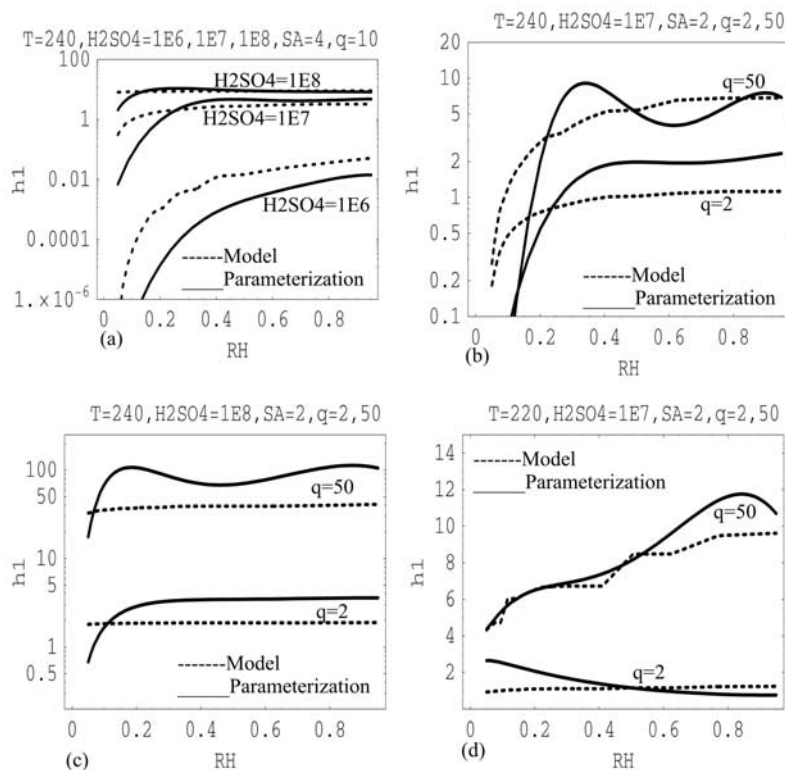


**Figure 6.** (a) Comparison of modeled and parameterized particle nucleation rate ( $h_1$ ) for  $T = 240$ ,  $\text{H}_2\text{SO}_4 = 10^6$ ,  $10^7$ , and  $10^8 \text{ cm}^{-3}$ ,  $\text{SA} = 4 \mu\text{m}^2 \text{ cm}^{-3}$ , and ion source equal to  $10 \text{ cm}^{-3} \text{ s}^{-1}$ . (b) Comparison of modeled and parameterized particle nucleation rate for  $T = 240$ ,  $\text{H}_2\text{SO}_4 = 10^7 \text{ cm}^{-3}$ ,  $\text{SA} = 2 \mu\text{m}^2 \text{ cm}^{-3}$ , and ion source equal to 2.0 and  $50.0 \text{ cm}^{-3} \text{ s}^{-1}$ . (c) Same as Figure 6b except for  $\text{H}_2\text{SO}_4 = 10^8 \text{ cm}^{-3}$ . (d) Same as Figure 6b except for  $T = 220$ .

their coefficients were computed by Mathematica programs. The sum of the squares of the offsets (difference between model and calculated value) is used instead of the offset absolute values because this allows the residuals to be treated as a continuous differentiable quantity. However, because squares of the offsets are used, outlying points can have a disproportionate effect on the fit, a property that is not desirable. For a number of unknown parameters, linear least squares fitting was applied iteratively to a linearized form of the function until convergence is achieved. Depending on the type of fit and initial parameters chosen, the nonlinear fit may have good or poor efficiency. If uncertainties (in the most general case, error ellipse) are given for the points, it can be weighted differently in order to give high-quality points more weight.

[15] Least squares fitting proceeded by finding the sum of the squares of the vertical deviations of a set of  $n$  data points from a function  $f$ . In addition, although the unsquared sum of distances might seem a more appropriate quantity to minimize, use of the absolute value results in discontinuous derivatives that cannot be treated analytically. The square deviations from each point are therefore summed, and the resulting residual is then minimized to find the best fit line. This procedure resulted in outlying points being given disproportionately large weighting and thus were eliminated iteratively. A reasonable fit with efficiencies exceeding 85% was obtained, in which the difference between the parameterized values and model values were well within an order of magnitude.

[16] The Vehkamäki *et al.* [2002] parameterization based on the classical nucleation model had four independent variables, namely  $T$ , RH,  $\text{H}_2\text{SO}_4$ , and  $h_3$  (number of  $\text{H}_2\text{SO}_4$  molecules in average nucleating cluster). Basis functions used in that parameterization were powers of  $\ln \text{RH}$ ,  $\ln \text{H}_2\text{SO}_4$ , beside  $1/h_3$ , and a series of cubic polynomials in  $T$ . We tried an IIN parameterization with a similar choice of basis functions, and obtained a good fit for  $h_1$  and  $h_2$ . The additional independent variables in this IIN parameterization namely,  $\text{SA}$  and  $q$ , were modeled with polynomials. This approach led to a more compact parameterization and is presented in this paper.

### 3.3. Parameterized Formulas

[17] The parameterized expressions for  $h_1$ ,  $h_2$ ,  $h_3$ ,  $h_4$  and  $h_5$  and their 3-D visualization as well as comparisons with corresponding model values are given in the supplementary material that will be made available on the Internet. The final parameterized formulas were taken directly from Mathematica; the FORTRAN forms for  $h_1$ ,  $h_2$ ,  $h_3$ ,  $h_4$ ,  $h_5$ , and  $h_6$  are given in the supplementary material. Expressions corresponding to C form (for those intending to use C programming language) can also be supplied on request.

## 4. Direct Comparison

[18] Figure 4 shows histograms of the frequency of occurrence as a function of the ratio of model value to the parameterization value for  $h_1$ ,  $h_2$ ,  $h_3$ ,  $h_4$  and  $h_5$ , respectively.

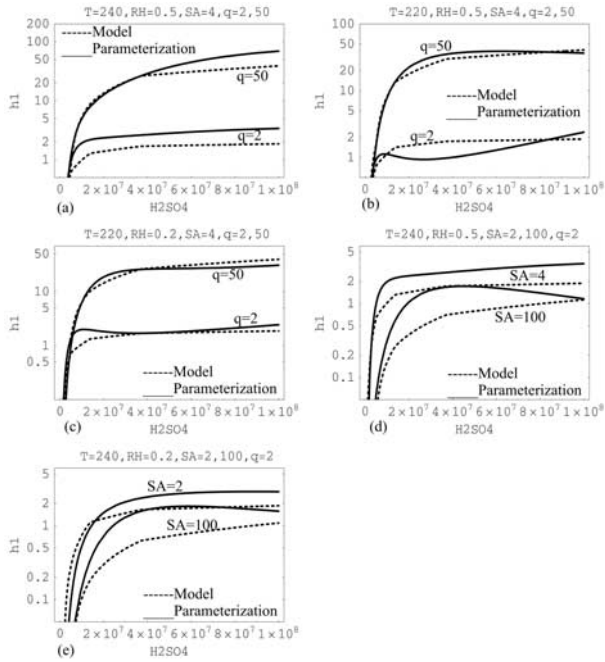


**Figure 7.** (a) Comparison of modeled and parameterized particle nucleation rate ( $h_1$ ) for  $T = 240$ ,  $RH = 0.5$ ,  $SA = 4 \mu\text{m}^2 \text{cm}^{-3}$ , and ion source equal to 2.0 and 50.0  $\text{cm}^{-3} \text{s}^{-1}$ . (b) Same as Figure 7a except for  $T = 220$ . (c) Same as Figure 7b except for  $RH = 0.2$ . (d) Comparison of modeled and parameterized particle nucleation rate for  $T = 240$ ,  $RH = 0.5$ ,  $SA = 2.0$  and  $100.0 \mu\text{m}^2 \text{cm}^{-3}$ , and ion source equal to 2.0  $\text{cm}^{-3} \text{s}^{-1}$ . (e) Same as Figure 7d except for  $RH = 0.2$ .

We define the efficiency as the percentage of points where the ratio of model value to the parameterized value falls between 0.5 and 2 for the conditions where  $h_1 > 10^{-6} \text{cm}^{-3} \text{s}^{-1}$ . Efficiencies exceeding 85% were obtained for particle nucleation rate ( $h_1$ ), nucleating  $\text{H}_2\text{SO}_4$  rate ( $h_3$ ), number of  $\text{H}_2\text{SO}_4$  molecules in average nucleating cluster ( $h_3$ ), number of  $\text{H}_2\text{O}$  molecules in average nucleating cluster ( $h_4$ ) and radius of nucleating cluster ( $h_5$ ).

[19] From Figure 5a, it can be seen that the parameterized particle nucleation rate ( $h_1$ ) is comparing well with model values, in the range,  $T = 190$ – $280$  K, and  $\text{H}_2\text{SO}_4 = 10^6$ – $10^7 \text{cm}^{-3}$ . Figure 5b shows that parameterized  $h_1$ , is within an order of magnitude for the range of  $T = 190$ – $236$  K, and  $\text{H}_2\text{SO}_4 = 10^5$  and  $10^8 \text{cm}^{-3}$ . However, for  $T > 236$  K and  $\text{H}_2\text{SO}_4 = 10^5$ , there is sudden drop in modeled  $h_1$  that is not well captured by parameterization, but at  $\text{H}_2\text{SO}_4 = 10^8 \text{cm}^{-3}$ , the modeled and parameterized values agree well. Figure 5b has a minimum around 202 K for the modeled curve. Several other curves also have “steps” versus temperature. These are caused by not accounting for the evaporation of neutral critical cluster in calculating the net IIN flux. However, this should not be serious issue, since a smooth curve through the calculated points should be close to reality.

[20] Figure 5c shows the effect of ion source on particle nucleation rate ( $h_1$ ), for  $q = 2$  and 50 ion pairs  $\text{cm}^{-3} \text{s}^{-1}$  at  $RH = 0.2$ ,  $\text{H}_2\text{SO}_4 = 10^7 \text{cm}^{-3}$  and  $SA = 2 \mu\text{m}^2 \text{cm}^{-3}$ . Figure 5d shows the same effect for  $\text{H}_2\text{SO}_4 = 10^8 \text{cm}^{-3}$  whereas Figure 5e shows the effect of  $q$  on particle nucleation rate at  $RH = 0.5$ ,  $SA = 2 \mu\text{m}^2 \text{cm}^{-3}$  and  $\text{H}_2\text{SO}_4 = 10^7 \text{cm}^{-3}$ .

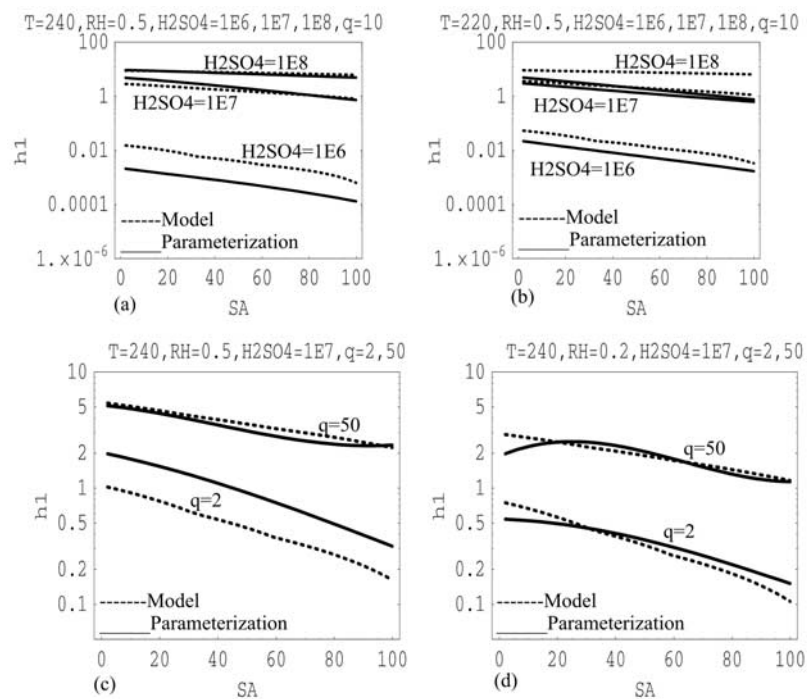


**Figure 8.** (a) Comparison of modeled and parameterized particle nucleation rate ( $h_1$ ) for  $T = 240$ ,  $RH = 0.5$ ,  $\text{H}_2\text{SO}_4 = 10^6$ ,  $10^7$ , and  $10^8 \text{cm}^{-3}$ , and ion source equal to 10.0  $\text{cm}^{-3} \text{s}^{-1}$ . (b) Same as Figure 8a except for  $T = 220$ . (c) Comparison of modeled and parameterized particle nucleation rate for  $T = 240$ ,  $RH = 0.5$ ,  $\text{H}_2\text{SO}_4 = 10^7 \text{cm}^{-3}$ , and ion source equal to 2.0 and 50.0  $\text{cm}^{-3} \text{s}^{-1}$ . (d) Same as Figure 8c except for  $RH = 0.2$ .

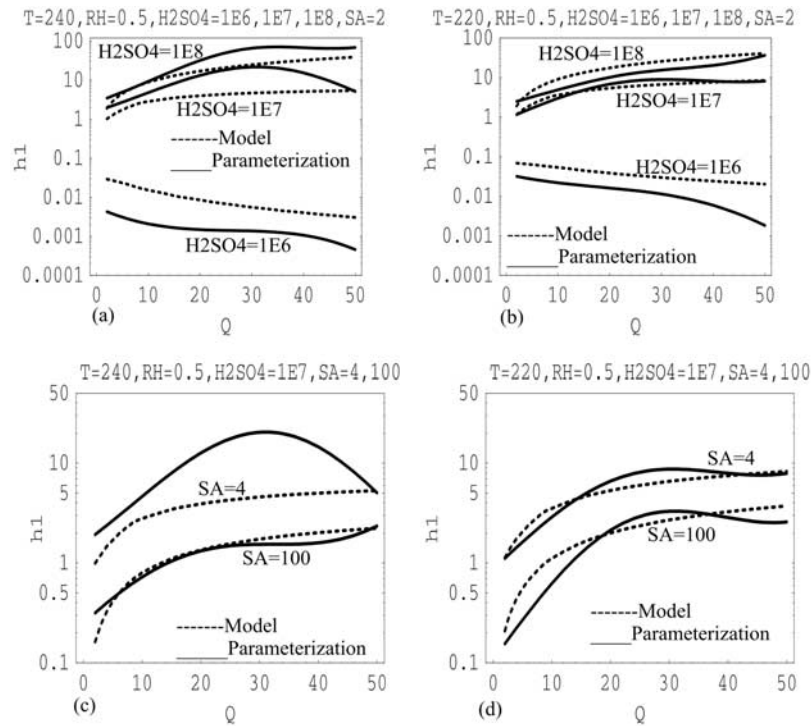


**Figure 9.** (a) Comparison of modeled and parameterized particle nucleation rate ( $h_1$ ) for  $T = 240$ ,  $\text{RH} = 0.5$ ,  $\text{H}_2\text{SO}_4 = 10^6, 10^7$ , and  $10^8 \text{ cm}^{-3}$ , and  $\text{SA} = 2 \mu\text{m}^2 \text{ cm}^{-3}$ . (b) Same as Figure 9a except for  $T = 220$ . (c) Comparison of modeled and parameterized particle nucleation rate for  $T = 240$ ,  $\text{RH} = 0.5$ ,  $\text{H}_2\text{SO}_4 = 10^7 \text{ cm}^{-3}$ , and  $\text{SA} = 4.0$  and  $100.0 \mu\text{m}^2 \text{ cm}^{-3}$ . (d) Same as Figure 9c except for  $T = 220$ .

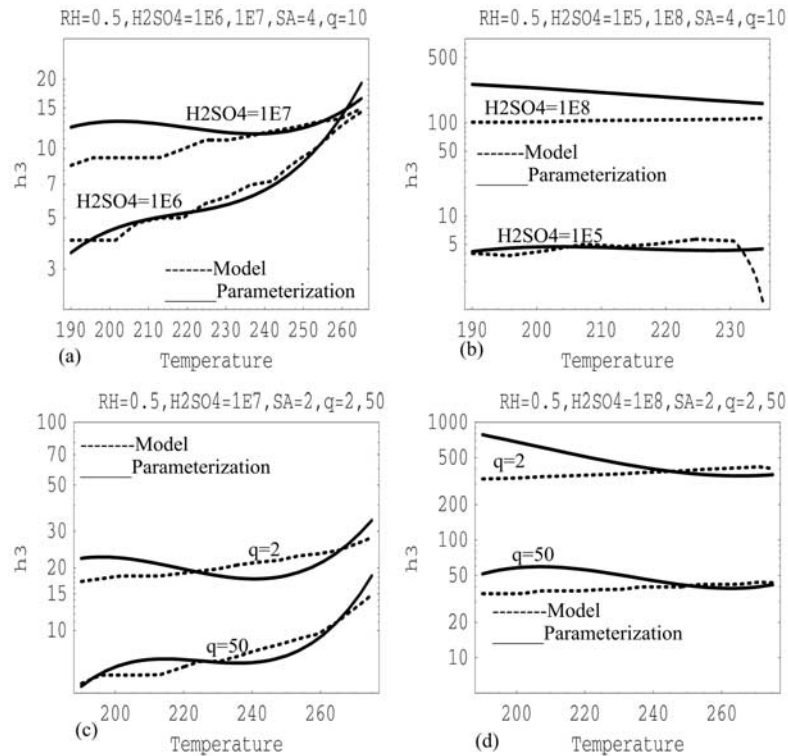


**Figure 10.** (a) Comparison of modeled and parameterized number of  $\text{H}_2\text{SO}_4$  molecules in average nucleating cluster ( $h_3$ ) for  $\text{RH} = 0.5$ ,  $\text{H}_2\text{SO}_4 = 10^6$  and  $10^7 \text{ cm}^{-3}$ ,  $\text{SA} = 4 \mu\text{m}^2 \text{ cm}^{-3}$ , and ion source equal to  $10 \text{ cm}^{-3} \text{ s}^{-1}$ . (b) Same as Figure 10a except for  $\text{H}_2\text{SO}_4 = 10^5$  and  $10^8 \text{ cm}^{-3}$ . (c) Comparison of modeled and parameterized number of  $\text{H}_2\text{SO}_4$  molecules in average nucleating cluster ( $h_3$ ) for  $\text{RH} = 0.5$ ,  $\text{H}_2\text{SO}_4 = 10^7 \text{ cm}^{-3}$ ,  $\text{SA} = 2 \mu\text{m}^2 \text{ cm}^{-3}$ , and ion source equal to  $2.0$  and  $50.0 \text{ cm}^{-3} \text{ s}^{-1}$ . (d) Same as Figure 10c except for  $\text{H}_2\text{SO}_4 = 10^8 \text{ cm}^{-3}$ .

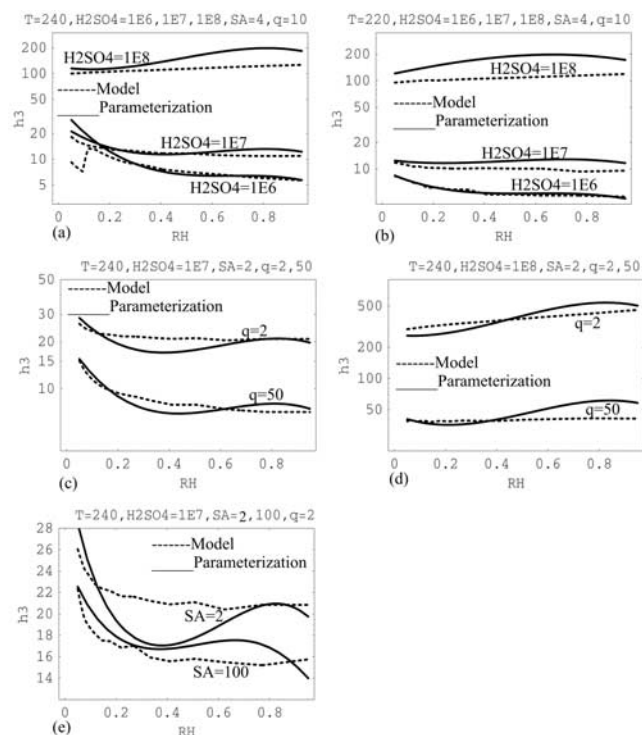


**Figure 11.** (a) Comparison of modeled and parameterized number of  $\text{H}_2\text{SO}_4$  molecules in average nucleating cluster ( $h_3$ ) for  $T = 240$ ,  $\text{H}_2\text{SO}_4 = 10^6$ ,  $10^7$ , and  $10^8 \text{ cm}^{-3}$ ,  $\text{SA} = 4 \mu\text{m}^2 \text{ cm}^{-3}$ , and ion source equal to  $10 \text{ cm}^{-3} \text{ s}^{-1}$ . (b) Same as Figure 11a except for  $T = 220$ . (c) Comparison of modeled and parameterized number of  $\text{H}_2\text{SO}_4$  molecules in average nucleating cluster ( $h_3$ ) for  $T = 240$ ,  $\text{H}_2\text{SO}_4 = 10^7 \text{ cm}^{-3}$ ,  $\text{SA} = 2 \mu\text{m}^2 \text{ cm}^{-3}$ , and ion source equal to 2.0 and  $50.0 \text{ cm}^{-3} \text{ s}^{-1}$ . (d) Same as Figure 11c except for  $\text{H}_2\text{SO}_4 = 10^8 \text{ cm}^{-3}$ . (e) Comparison of modeled and parameterized particle nucleation rate for  $T = 240$ ,  $\text{H}_2\text{SO}_4 = 10^7 \text{ cm}^{-3}$ , ion source equal to  $2 \text{ cm}^{-3} \text{ s}^{-1}$ , and  $\text{SA} = 2.0$  and  $100.0 \mu\text{m}^2 \text{ cm}^{-3}$ .

[21] Figure 5c shows that modeled and parameterized particle nucleation rate ( $h_1$ ) agree well up to  $T = 250 \text{ K}$ . It is evident from Figure 5d that parameterized  $h_1$  is capturing model trend and values are within an order of magnitude except at low temperatures for two different ion source rates. Figure 5e shows that parameterized  $h_1$  are in good agreement with modeled one except at low temperatures and  $q = 50$  ion pairs. Similar plots (Figures 6–9) show the dependence of  $h_1$  on RH,  $\text{H}_2\text{SO}_4$ , SA and  $q$  as well as the direct comparison between modeled and parameterized  $h_1$ .

[22] Figures 10a and 10b show the effect of  $\text{H}_2\text{SO}_4$  on number of  $\text{H}_2\text{SO}_4$  molecules in average nucleating cluster ( $h_3$ ) at  $\text{RH} = 0.5$ ,  $\text{SA} = 4$ ,  $q = 10$  and  $\text{H}_2\text{SO}_4 = 10^6$  and  $10^7$ ,  $10^5$  and  $10^8 \text{ cm}^{-3}$ , respectively. From Figure 10a, it can be seen that parameterized  $h_3$  compares well with model values, in the range,  $T = 190$ – $270 \text{ K}$ . Figure 10b shows that parameterized  $h_3$ , is within an order of magnitude for the range,  $T = 190$ – $230 \text{ K}$ . However, for  $T > 230 \text{ K}$  and at  $\text{H}_2\text{SO}_4 = 10^5$ , there is sudden drop in model values which is not captured by parameterization but at  $\text{H}_2\text{SO}_4 = 10^8 \text{ cm}^{-3}$  the match in model and parameterized

values is reasonable for the range of temperature considered here.

[23] Figures 10c and 10d show the effects of  $q$  on number of  $\text{H}_2\text{SO}_4$  molecules in average nucleating cluster ( $h_3$ ) at  $\text{SA} = 2$ ,  $q = 2, 50$  at different  $\text{H}_2\text{SO}_4$ . Except in the low-temperature region, the parameterization agrees well with model values for both the cases of ion source. Overall, it can be seen that the parameterization is able to reproduce the trend of model and the values of parameterized number of  $\text{H}_2\text{SO}_4$  molecules in average nucleating cluster ( $h_3$ ) are within an order of magnitude for full temperature range. Similar plots (Figures 11–14) show the dependence of  $h_3$  on RH,  $\text{H}_2\text{SO}_4$ , SA and  $q$  as well as the direct comparison between modeled and parameterized  $h_3$ .

[24] Figures 15a and 15b show the effect of  $\text{H}_2\text{SO}_4$  on radius of nucleating cluster ( $h_5$ ) at  $\text{RH} = 0.5$ ,  $\text{SA} = 4$ ,  $q = 10$  and  $\text{H}_2\text{SO}_4 = 10^6$  and  $10^7$ ,  $10^5$  and  $10^8 \text{ cm}^{-3}$ , respectively. From Figure 15a, it can be seen that parameterized  $h_5$  is comparing well with model values, in the range,  $T = 190$ – $270 \text{ K}$  except a sudden drop in modeled  $h_5$  at  $T > 265$  and  $\text{H}_2\text{SO}_4 = 10^6 \text{ cm}^{-3}$ , which is not captured by parameterization. Figure 15b shows that parameterized  $h_5$ , is within an order of magnitude of the model values for the range,  $T = 190$ – $230 \text{ K}$ . At  $T > 230 \text{ K}$  and at  $\text{H}_2\text{SO}_4 = 10^5$ , parameterization fails to capture the model trends but at  $\text{H}_2\text{SO}_4 = 10^8 \text{ cm}^{-3}$ , the match in model and parameterized values is reasonable for  $T = 190$ – $240 \text{ K}$ .

[25] Figures 15c–15e show the effect of ion source on radius of nucleating cluster ( $h_5$ ) at  $\text{SA} = 2$ ,  $q = 2, 50$  and at different  $\text{H}_2\text{SO}_4$  and RH combinations. Figure 15d shows similar effect for  $\text{H}_2\text{SO}_4 = 10^8 \text{ cm}^{-3}$ . Except in the low-temperature region, the parameterization agrees well with model values for both the cases of ion source. Figure 15e shows the effect of ion source on  $h_5$  at  $\text{RH} = 0.5$ ,  $\text{SA} = 2 \mu\text{m}^2 \text{ cm}^{-3}$  and  $\text{H}_2\text{SO}_4 = 10^7 \text{ cm}^{-3}$ . It can also be seen that the parameterization is capturing the trend of model and the values of parameterized  $h_5$  are within an order of magnitude for  $T = 190$ – $270 \text{ K}$ . Similar plots (Figures 16–19) show the dependence of  $h_5$  on RH,  $\text{H}_2\text{SO}_4$ , SA and  $q$  as well as the direct comparison between modeled and parameterized  $h_5$ .

## 5. Summary and Conclusions

[26] This paper presents a parameterization of IIN for atmospheric conditions. It uses a kinetic aerosol model SAWNUC [Lovejoy *et al.*, 2004], which is based upon measured thermodynamics of ion cluster growth. It is shown that the steady state ion-induced nucleation rate is a very good approximation to the instantaneous rate. Accordingly, data for the parameterization were generated by running a steady state version of SAWNUC over a wide range of atmospheric conditions. The parameterization speeds up the calculations by a factor of about  $10^6$  and is useful for implementation in large-scale models.

[27] Comparison between model and parameterized values is well within an order of magnitude, for most range of conditions. The standard deviation of the ratio of model values and corresponding parameterized values, which should be ideally unity, is a measure of deviation of the parameterization from model. The standard deviation for the ratio of model values to the parameterized values lies

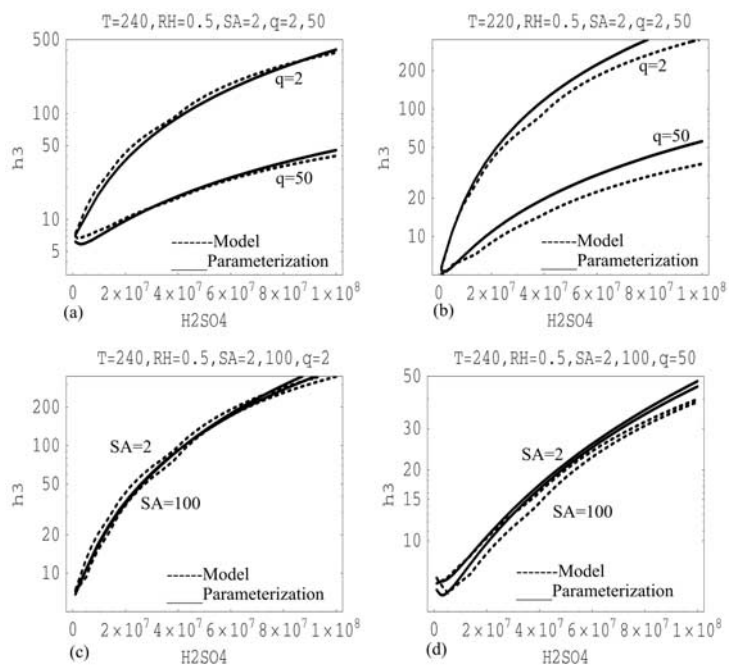


**Figure 12.** (a) Comparison of modeled and parameterized number of  $\text{H}_2\text{SO}_4$  molecules in average nucleating cluster ( $h_3$ ) for  $T = 240$ ,  $\text{RH} = 0.5$ ,  $\text{SA} = 2 \mu\text{m}^2 \text{cm}^{-3}$ , and ion source equal to 2.0 and 50.0  $\text{cm}^{-3} \text{s}^{-1}$ . (b) Same as Figure 12a except for  $T = 220$ . (c) Comparison of modeled and parameterized number of  $\text{H}_2\text{SO}_4$  molecules in average nucleating cluster ( $h_3$ ) for  $T = 240$ ,  $\text{RH} = 0.5$ , ion source equal to 2.0, and  $\text{SA} = 2.0$  and  $100.0 \mu\text{m}^2 \text{cm}^{-3}$ . (d) Same as Figure 12c except for ion source equal to 50  $\text{cm}^{-3} \text{s}^{-1}$ .

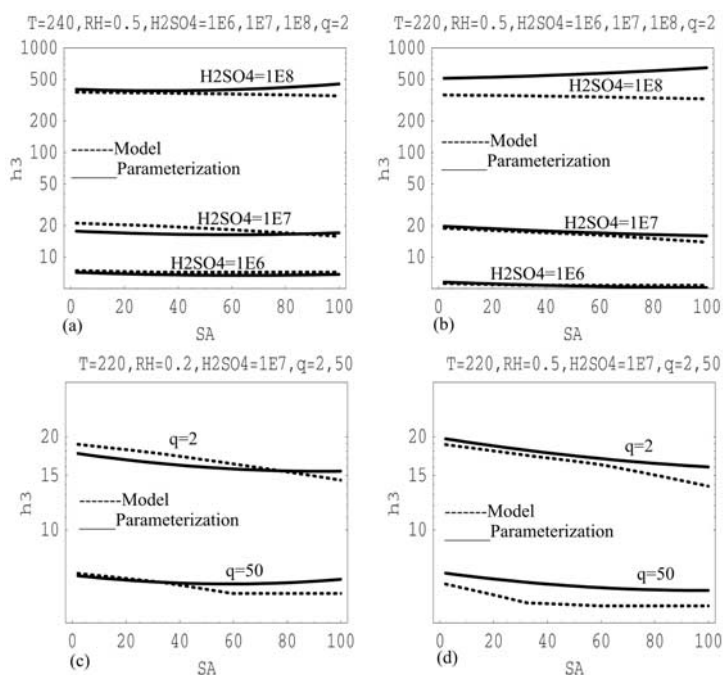


**Figure 13.** (a) Comparison of modeled and parameterized number of  $\text{H}_2\text{SO}_4$  molecules in average nucleating cluster ( $h_3$ ) for  $T = 240$ ,  $\text{RH} = 0.5$ ,  $\text{H}_2\text{SO}_4 = 10^6, 10^7, \text{ and } 10^8 \text{ cm}^{-3}$ , and ion source equal to 2.0  $\text{cm}^{-3} \text{s}^{-1}$ . (b) Same as Figure 13a except for  $T = 220$ . (c) Comparison of modeled and parameterized number of  $\text{H}_2\text{SO}_4$  molecules in average nucleating cluster ( $h_3$ ) for  $T = 220$ ,  $\text{RH} = 0.2$ ,  $\text{H}_2\text{SO}_4 = 10^7 \text{ cm}^{-3}$ , and ion source equal to 2.0 and 50.0  $\text{cm}^{-3} \text{s}^{-1}$ . (d) Same as Figure 13c except for  $\text{RH} = 0.5$ .

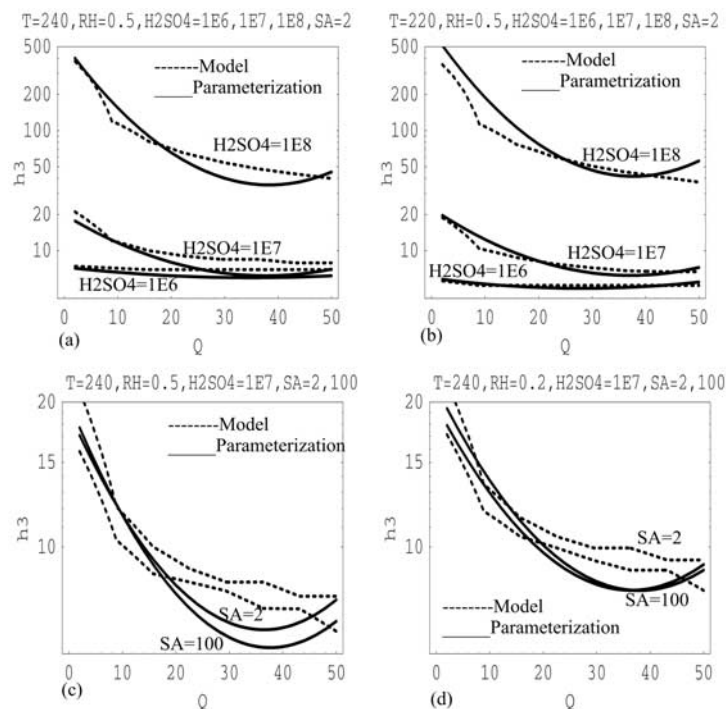


**Figure 14.** (a) Comparison of modeled and parameterized number of  $\text{H}_2\text{SO}_4$  molecules in average nucleating cluster ( $h_3$ ) for  $T = 240$ ,  $\text{RH} = 0.5$ ,  $\text{H}_2\text{SO}_4 = 10^6$ ,  $10^7$ , and  $10^8 \text{ cm}^{-3}$ , and  $\text{SA} = 2 \mu\text{m}^2 \text{ cm}^{-3}$ . (b) Same as Figure 14a except for  $T = 220$ . (c) Comparison of modeled and parameterized number of  $\text{H}_2\text{SO}_4$  molecules in average nucleating cluster ( $h_3$ ) for  $T = 240$ ,  $\text{RH} = 0.5$ ,  $\text{H}_2\text{SO}_4 = 10^7 \text{ cm}^{-3}$ , and  $\text{SA} = 2.0$  and  $100.0 \mu\text{m}^2 \text{ cm}^{-3}$ . (d) Same as Figure 14c except for  $\text{RH} = 0.2$ .

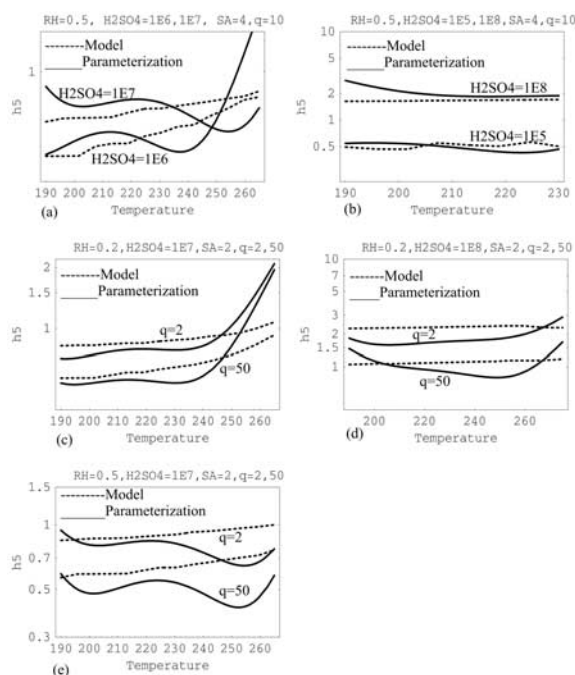


**Figure 15.** (a) Comparison of modeled and parameterized radius (nanometers) of average nucleating cluster ( $h_5$ ) for  $\text{RH} = 0.5$ ,  $\text{H}_2\text{SO}_4 = 10^6$  and  $10^7 \text{ cm}^{-3}$ ,  $\text{SA} = 4 \mu\text{m}^2 \text{ cm}^{-3}$ , and ion source equal to  $10 \text{ cm}^{-3} \text{ s}^{-1}$ . (b) Same as Figure 15a except for  $\text{H}_2\text{SO}_4 = 10^5$  and  $10^8 \text{ cm}^{-3}$ . (c) Comparison of modeled and parameterized radius (nanometers) of average nucleating cluster ( $h_5$ ) for  $\text{RH} = 0.2$ ,  $\text{H}_2\text{SO}_4 = 10^7 \text{ cm}^{-3}$ ,  $\text{SA} = 2 \mu\text{m}^2 \text{ cm}^{-3}$ , and ion source equal to 2 and  $50 \text{ cm}^{-3} \text{ s}^{-1}$ . (d) Same as Figure 15c except for  $\text{H}_2\text{SO}_4 = 10^8 \text{ cm}^{-3}$ . (e) Same as Figure 15c except for  $\text{RH} = 0.5$ .

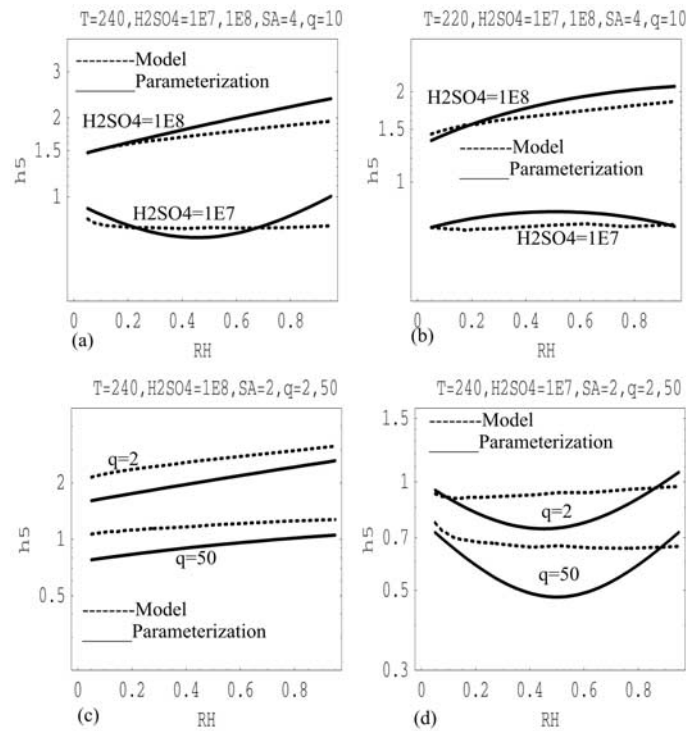


**Figure 16.** (a) Comparison of modeled and parameterized radius (nanometers) of average nucleating cluster ( $h_5$ ) for  $T = 240$ ,  $\text{H}_2\text{SO}_4 = 10^7$  and  $10^8 \text{ cm}^{-3}$ ,  $\text{SA} = 4 \mu\text{m}^2 \text{ cm}^{-3}$ , and ion source equal to  $10 \text{ cm}^{-3} \text{ s}^{-1}$ . (b) Same as Figure 16a except for  $T = 220$ . (c) Comparison of modeled and parameterized radius (nanometers) of average nucleating cluster ( $h_5$ ) for  $T = 240$ ,  $\text{H}_2\text{SO}_4 = 10^8 \text{ cm}^{-3}$ ,  $\text{SA} = 2 \mu\text{m}^2 \text{ cm}^{-3}$ , and ion source equal to 2 and  $50 \text{ cm}^{-3} \text{ s}^{-1}$ . (d) Same as Figure 16c except for  $\text{H}_2\text{SO}_4 = 10^7 \text{ cm}^{-3}$ .

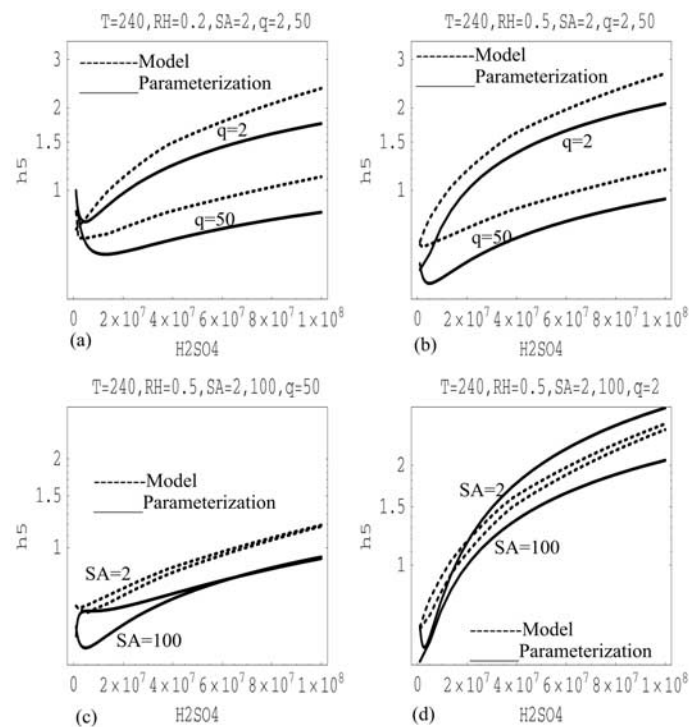


**Figure 17.** (a) Comparison of modeled and parameterized radius (nanometers) of average nucleating cluster ( $h_5$ ) for  $T = 240$ ,  $\text{RH} = 0.2$ ,  $\text{SA} = 2.0 \mu\text{m}^2 \text{ cm}^{-3}$ , and ion source equal to 2.0 and  $50.0 \text{ cm}^{-3} \text{ s}^{-1}$ . (b) Same as Figure 17a except for  $\text{RH} = 0.5$ . (c) Comparison of modeled and parameterized radius (nanometers) of average nucleating cluster ( $h_5$ ) for  $T = 240$ ,  $\text{RH} = 0.5$ , ion source equal to  $50.0 \text{ cm}^{-3} \text{ s}^{-1}$ , and  $\text{SA} = 2.0$  and  $100.0 \mu\text{m}^2 \text{ cm}^{-3}$ . (d) Same as Figure 17c except for ion source equal to  $2.0 \text{ cm}^{-3} \text{ s}^{-1}$ .

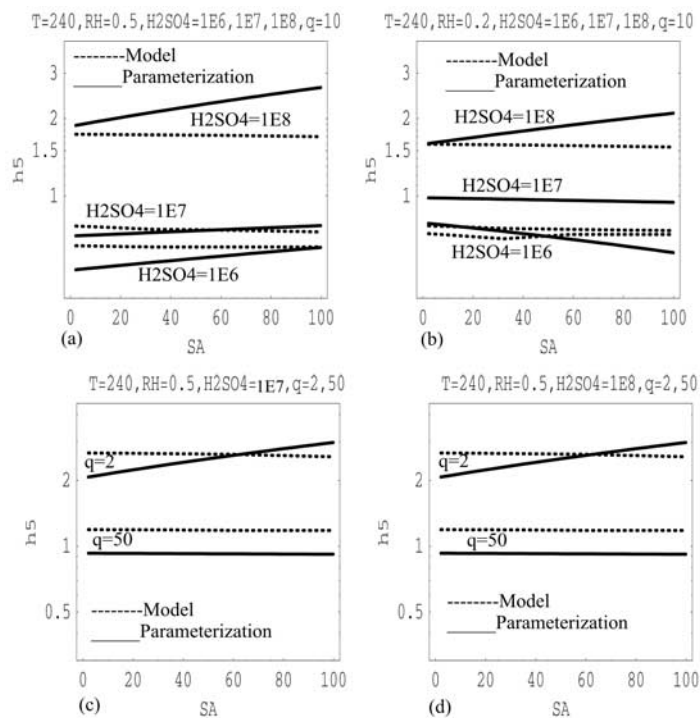


**Figure 18.** (a) Comparison of modeled and parameterized radius (nanometers) of average nucleating cluster ( $h_5$ ) for  $T = 240$ ,  $RH = 0.5$ ,  $H_2SO_4 = 10^6$ ,  $10^7$ , and  $10^8$   $cm^{-3}$ , and ion source equal to  $10$   $cm^{-3} s^{-1}$ . (b) Same as Figure 18a except for  $RH = 0.2$ . (c) Comparison of modeled and parameterized radius (nanometers) of average nucleating cluster ( $h_5$ ) for  $T = 240$ ,  $RH = 0.5$ ,  $H_2SO_4 = 10^7$   $cm^{-3}$ , and ion source equal to  $2.0$  and  $50.0$   $cm^{-3} s^{-1}$ . (d) Same as Figure 18c except for  $H_2SO_4 = 10^8$   $cm^{-3}$ .

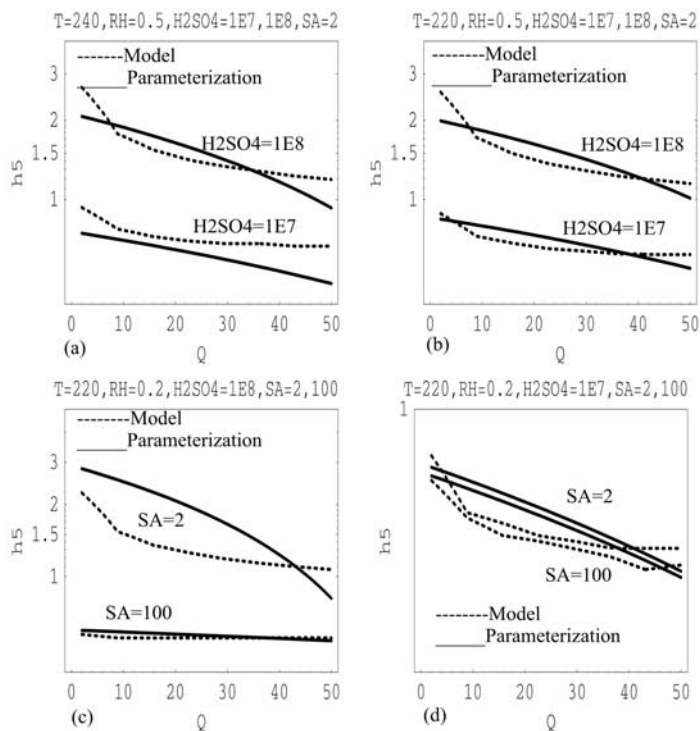


**Figure 19.** (a) Comparison of modeled and parameterized radius (nanometers) of average nucleating cluster ( $h_5$ ) for  $T = 240$ ,  $RH = 0.5$ ,  $H_2SO_4 = 10^7$  and  $10^8$   $cm^{-3}$ , and  $SA = 2$   $\mu m^2 cm^{-3}$ . (b) Same as Figure 19a except for  $T = 220$ . (c) Comparison of modeled and parameterized radius (nanometers) of average nucleating cluster ( $h_5$ ) for  $T = 220$ ,  $RH = 0.2$ ,  $H_2SO_4 = 10^8$   $cm^{-3}$ , and  $SA = 2.0$  and  $100.0$   $\mu m^2 cm^{-3}$ . (d) Same as Figure 19c except for  $H_2SO_4 = 10^7$   $cm^{-3}$ .

between 0.22 and 0.57. The exceptions occur for the following conditions: (1) when the particle nucleation rate is very low ( $<10^{-6}$ ), which corresponds to a rate of less than 0.1 particle  $d^{-1}$ , (2) extreme conditions, e.g., very low or high values of temperature, relative humidity,  $H_2SO_4$ , etc. It is noticed that gradients (slopes) of model and parameterized values generally match, except when the model has steep slopes immediately followed by plateaus. This may be because polynomials of cubic order in temperature were used in this parameterization. Higher-degree polynomials may capture the model behavior better at the cost of more computational resources and bulkier expressions. These IIN parameterization functions are presently being used in an aerosol microphysical model to interpret the particle formation observations, which are not explained by classical nucleation theory.

[28] **Acknowledgments.** S.N.T., M.S.M., and S.K. are supported through a research grant from the RESPOND Program of the Indian Space Research Organization. This work was supported in part by the NOAA Climate and Global Change Program. The authors acknowledge useful discussions with Jan Kazil.

## References

- Froyd, K. D., and E. R. Lovejoy (2003a), Experimental thermodynamics of cluster ions composed of  $H_2SO_4$  and  $H_2O$ : 1. Positive ions, *J. Phys. Chem. A*, *107*, 9800–9811.
- Froyd, K. D., and E. R. Lovejoy (2003b), Experimental thermodynamics of cluster ions composed of  $H_2SO_4$  and  $H_2O$ : 2. Negative ions, *J. Phys. Chem. A*, *107*, 9812–9824.
- Kim, T. O., M. Adachi, K. Okuyama, and J. Seinfeld (1997), Experimental measurement of competitive ion-induced and binary homogenous nucleation  $SO_2/H_2O/N_2$  mixtures, *Aerosol Sci. Technol.*, *26*, 527–543.
- Kulmala, M. (2003), How particles nucleate and grow, *Science*, *302*, 1000–1001.
- Kulmala, M., L. Pirjola, and J. M. Mäkelä (2000), Stable sulfate clusters as a source of new atmospheric particles, *Nature*, *404*, 66–69.
- Laakso, L., J. M. Mäkelä, L. Pirjola, and M. Kulmala (2002), Model studies on ion-induced nucleation in the atmosphere, *J. Geophys. Res.*, *107*(D20), 4427, doi:10.1029/2002JD002140.
- Lee, S. H., J. M. Reeves, J. C. Wilson, D. E. Hunton, A. A. Viggiano, T. M. Miller, J. O. Ballenthin, and L. R. Lait (2003), Particle formation by ion nucleation in the upper troposphere and lower stratosphere, *Science*, *301*, 1886–1889.
- Lovejoy, E. R., J. Curtius, and K. D. Froyd (2004), Atmospheric ion-induced nucleation of sulfuric acid and water, *J. Geophys. Res.*, *109*, D08204, doi:10.1029/2003JD004460.
- Napari, I., M. Noppel, H. Vehkamäki, and M. Kulmala (2002), Parameterization of ternary nucleation rates for  $H_2SO_4$ - $NH_3$ - $H_2O$  vapors, *J. Geophys. Res.*, *107*(D19), 4381, doi:10.1029/2002JD002132.
- Raes, F., and A. Janssens (1986), Ion-induced aerosol formation in a  $H_2O$ - $H_2SO_4$  system: II. Numerical calculations and conclusions, *J. Aerosol. Sci.*, *17*, 715–722.
- Seinfeld, J. H., and S. N. Pandis (1998), *Atmospheric Chemistry and Physics*, John Wiley, Hoboken, N. J.
- Vehkamäki, H., M. Kulmala, I. Napari, K. E. J. Lehtinen, C. Timmreck, M. Noppel, and A. Laaksonen (2002), An improved parameterization for sulfuric acid–water nucleation rates for tropospheric and stratospheric conditions, *J. Geophys. Res.*, *107*(D22), 4622, doi:10.1029/2002JD002184.
- Wilhelm, S., S. Eichkorn, D. Wiedner, L. Pirjola, and F. Arnold (2004), Ion-induced aerosol formation: New insights from laboratory measurements of mixed cluster ions  $HSO_4^-(H_2SO_4)_{(a)}(H_2O)_{(w)}$  and  $H^+(H_2SO_4)_{(a)}(H_2O)_{(w)}$ , *Atmos. Environ.*, *38*, 1735–1744.
- Yu, F., and R. P. Turco (2000), Ultrafine aerosol formation via ion-mediated nucleation, *Geophys. Res. Lett.*, *27*(6), 883–886.
- Yu, F., and R. P. Turco (2001), From molecular clusters to nanoparticles: Role of ambient ionization in tropospheric aerosol formation, *J. Geophys. Res.*, *106*, 4797–4814.

S. Kumar and S. N. Tripathi, Department of Civil Engineering, Indian Institute of Technology, Kanpur 208 016 (UP), India. (snt@iitk.ac.in)  
 E. R. Lovejoy, NOAA Aeronomy Laboratory, 325 Broadway, Boulder, CO 80305, USA.  
 M. S. Modgil, Department of Physics, Indian Institute of Technology, Kanpur 208 016 (UP), India.